THE UNIVERSITY OF ALABAMA® | University Libraries

A Distribution-free Phase II Control Chart for Multivariate Individual Data with Simple Post Signal Diagnostics

Chakraborti, Subha-The University of Alabama
Alqurashi, Mosab- The University of Alabama
Holcombe, Chase- The University of South Alabama

Deposited 11/01/2024

This is an accepted manuscript published by Taylor and Francis Group in the *Quality Engineering* published February 13, 2024, available at: https://doi.org/10.1080/08982112.2024.2311253

Citation of published version:

Holcombe, C., Alqurashi, M., & Chakraborti, S. (2024). A distribution-free phase II control chart for multivariate individual data with simple post signal diagnostics. Quality Engineering, 36(4), 845–865. https://doi.org/10.1080/08982112.2024.2311253

© 2024 Taylor & Francis. This work is licensed under a CC BY-NC 4.0 license.

A Distribution-free Phase II Control Chart for Multivariate Individual Data with Simple Post Signal Diagnostics

Chase Holcombe[1], Mosab Alqurashi[2] and Subhabrata Chakraborti[1]

This is an Accepted Manuscript of an article published by Taylor & Francis in Quality Engineering on 13 February 2024, available at: https://doi.org/10.1080/08982112.2024.2311253

Abstract

Multivariate statistical process control (MSPC) charts are particularly useful when there is a need to simultaneously monitor several quality characteristics of a process. Most of the control charts in MSPC assume that the quality characteristics follow some parametric multivariate distribution, such as the normal. This assumption is almost impossible to be justified in practice. Distribution-free MSPC charts are attractive, as they can overcome this hurdle by guaranteeing a stable (or in-control (IC)) performance of the control chart without the assumption of a parametric multivariate process distribution. Utilizing an existing distribution-free multivariate tolerance interval, we propose a Phase II Shewhart-type distribution-free MSPC chart for individual observations, with control limits based on Phase I order statistics. In addition to being easy to interpret, the proposed chart preserves the original scale of measurements and can easily identify out-of-control variables after a signal. The exact in-control performance based on the conditional and unconditional perspectives is presented and examined along with the control limits determination. The out-of-control performance of the chart is studied by simulation for data from a number of multivariate distributions. Illustrative examples are provided for chart implementation, using both real and simulated data, along with a summary and conclusions.

Keywords: Multivariate control chart, nonparametric, Phase I and II charts for process monitoring, order statistics, tolerance regions, conditional and unconditional perspectives, simulation.

[1] Department of Information Systems, Statistics and Management Science, University of Alabama, Tuscaloosa, AL 35487, U.S.A.

[2] Department of Quantitative Analysis, King Saud University, Riyadh, Saudi Arabia 11451

1 Introduction

Many of the popular statistical process control (SPC) charts assume that the quality characteristic being controlled/monitored follows some parametric distribution. In practice, this assumption is rarely, if ever, satisfied and as a result the inference drawn from the charts might be incorrect, especially when monitoring individual observations in the multivariate setting. An alternative approach is to use distribution-free control charts. A control chart is distribution-free if its IC run length distribution is the same for all continuous process distributions as defined by Chakraborti et al. (2004). Recently published books by Chakraborti and Graham (2019a) and Koutras and Triantafyllou (2020) detail many of the available distribution-free control charts in the univariate and multivariate cases. For additional information on the distribution-free methodology in the process monitoring setting, see Chakraborti (2014) and Chakraborti et al. (2015).

In recent years, there has been increased technological capabilities in the industrial world as well as an increase in the complexity of the production processes. In this environment, it often makes more sense that multiple characteristics of a process be monitored simultaneously. Given the fact that simultaneous monitoring of multiple related characteristics may not be as efficient and may be misleading when the characteristics are monitored independently, multivariate statistical process control (MSPC) methods are needed. Consequently, many methods for constructing multivariate control charts have been developed and proposed in the literature. See Bersimis et al. (2007) and Qiu (2014) for an overview of multivariate Shewhart, EWMA, CUSUM, and projection-based charts in the parametric setting. However, similar to the traditional univariate SPC, parametric MSPC typically assumes a multivariate process distribution, such as the multivariate normal, which is almost impossible to be justified in practice; in fact, the justification of normality is even harder in the multivariate case than the univariate case. For this reason, various multivariate distribution-free charts have been introduced in the literature. Notable reviews include those from Ge and Song (2013), Qiu (2018), and Chakraborti and Graham (2019b). Some authors have also constructed similar control schemes using a change point formulation (Zhou et al., 2015). See these papers for a recent and broad overview of distribution-free multivariate monitoring schemes with comparisons to parametric competitors.

For many of the existing MSPC charts, however, the post signal diagnostics remain an important practical issue. This means that the control charts may signal a change in the overall quality of the process, but one may not necessarily be able to pinpoint the variable(s) that caused the signal. Furthermore, some of the available control charts involve dimension reduction and/or projection based techniques, which usually cause the scale and the identity of the original variables to be lost, see Qin (2012). This exacerbates the difficulty in post-signal diagnostics. Note that some work has been done in the parametric setting to help with the post-signal interpretation. To this end, one important example is the T^2 chart introduced by Mason et al. (1995), for the multivariate normal distribution, which used partitioning or decomposition to aid in the interpretability. However, as Wu et al. (2023) recently pointed out, this method is computationally complex and the "T^2 decomposition has no clear physical meaning, which makes it difficult to detect the root cause of the problem." Bersimis et al. (2017) considered a number of multivariate parametric monitoring schemes and concluded that for diagnosing the component responsible for a signal, "there is no particular method that can be considered as panacea." In any case, as noted before, since the assumption of a multivariate normal process distribution can be next to impossible to justify in practice, it points to an important gap, that is, the need for some simple distribution-free multivariate control charts which may be more useful in practical applications.

In this paper, we consider a distribution-free Phase II Shewhart-type control chart to monitor a change in the process location parameter. This control scheme is designed to be applied to individual observations from a continuous process in the important case where the underlying parameters are unknown (so called case U) and where the control limits are estimated from an IC (Phase I or reference) sample. The goal is to monitor the process online (Phase II), to ensure that the process operates in a stable state (remains IC). Being a Shewhart-type chart of the data, the proposed chart is easy to implement, interpret and preserves the original scale of measurements. Moreover, the chart is exactly distribution-free, and can pinpoint the variables that cause the out-of-control (OOC) signal (so that post signal diagnostics are straightforward). Performance of the proposed chart is studied and to this end, the exact distributions of the conditional and unconditional IC run length are derived. From these, formulas for the sample size

requirement to achieve a particular performance measure such as a guaranteed average run length, are provided. This allows construction of the control chart according to two common perspectives used in the estimated parameter case, namely the conditional and the unconditional (Jardim et al., 2020). The OOC performance and comparisons are studied via simulation, since the OOC run length distribution is not distribution-free.

The proposed multivariate control chart can be viewed as a generalization of the univariate two-sided distribution-free control charts considered by Willemain and Runger (1996) and Chakraborti et al. (2004), which are designed to monitor a change in location. These are among the simplest and earliest distribution-free control charts based on order statistics. To this end, we utilize an implicit connection between control charts and tolerance intervals (TIs), both of which are useful tools in SPC applications. Recall that the TIs are random intervals that guarantee that the area "under the probability density function and between the endpoints" of the interval is at least some value p with probability γ (Gibbons and Chakraborti, 2020). This area, which is the probability that an observation from the same population will fall between the lower and upper tolerance limits constructed from an independent random sample, is referred to as the content of a TI (Krishnamoorthy and Mathew, 2009). In the charting context, the content corresponds to the probability of the so-called non-signaling event (that is when the chart does not signal) for a two-sided control chart when the process is IC. This connects a TI to a two-sided Shewhart-type control chart, to be discussed later. Similar connections have been made, that is, to use tolerance intervals to set up control limits, in the literature for the univariate case. Notably, Hamada (2002, 2003) used this connection to set up tolerance interval-based control limits for attribute charts and for $\bar{X}$, R, and S charts, respectively. We make use of this important connection to develop the proposed multivariate control chart.

The remainder of this paper is organized as follows: In Section 2, we first introduce the bivariate case (Section 2.1), derive the false alarm rate (Section 2.1) and the run length distribution (Section 2.2), demonstrate the control limit determination (Section 2.3), consider some selection criteria for the charting constants (Section 2.4), and demonstrate basic chart construction (Section 2.5). Performance measures are specifically considered when the practitioner is in the position to determine the Phase I sample size m (Section 2.6). Next, in

Section 3, we extend the method to the more general p-dimensional (multivariate) case (Sections 3.1 and 3.2), showing that the false alarm rate and run length distributions do not depend on the dimension p, which is an important advantage of the proposed methodology. The method for the control limit determination is generalized to the p-dimensional case (Section 3.3). The OOC performance is studied in Section 4 and multiple illustrative examples are presented in Section 5. Finally, some conclusions are offered in Section 6.

The bivariate case is considered first to set the stage.

2 The Bivariate Case

2.1 The Setting

Wald (1943) developed a distribution-free multivariate TI based on order statistics. In the bivariate case, this method constructs the tolerance region using m iid observations from a continuous distribution, using some indices a, b, c, and d. Remarkably, Wald's procedure results in a tolerance region that has probability content Q, where Wald (1943) showed that $Q \sim Beta(d-c, m-(d-c)+1)$, regardless of the underlying data distribution. In the process monitoring setting, the TI setting is analogous to the IC case. Thus, for the proposed control chart, we utilize this result to construct a control region. To this end, the distribution of Q is used and related to the IC signal probability (the false alarm rate), the run length distribution, and the conditional average run length distribution. First, in this section, we detail the background and the method for constructing the tolerance or control region in the bivariate case, tailored to the process monitoring setting.

Assume that we have m iid observations on a random vector (X_1, X_2) $\left((X_{1,1}, X_{2,1}), (X_{1,2}, X_{2,2}), \dots, (X_{1,m}, X_{2,m})\right)$ from an IC bi-variate process, where $X_{i,j}$ denotes the j^{th} observation of the i^{th} component, $i = 1,2,\ j = 1,2, \dots m$. These IC (reference) observations constitute a Phase I sample. The issue of finding a reference (Phase I) sample from a Phase I analysis is an interesting problem in itself, for more information, the reader can refer to the literature (see reviews by Chakraborti et al., 2008 and Jones-Farmer et al., 2014). Let L_1 denote the $a-th$ order statistic and M_1 denote the $b-th$ order statistic of the component X_1, respectively, so that $L_1 = X_{1,(a:m)}$ and $M_1 = X_{1,(b:m)}$. Thus, $b-a-1$ represents the number

of X_1 observations that lie strictly between L_1 and M_1. Let S denote the set containing these $b - a - 1$ observations and let the observations on the component X_2 that are among the observations in S (that is, their corresponding X_1 values lie strictly between L_1 and M_1) be denoted as X_2^*. Further let L_2 and M_2 denote the $c - th$ and $d - th$ order statistics of these X_2 observations, respectively, so that $L_2 = X^*_{2,(c:b-a-1)}$ and $M_2 = X^*_{2,(d:b-a-1)}$. Note that the values a, b, c, d are constrained such that:

$$1 \leq a < b \leq m \text{ and } 1 \leq c < d \leq b - a - 1 \quad (1)$$

From the definitions of the control limits, it is clear that $d - c - 1$ represents the number of X_2^* observations that lie strictly between L_2 and M_2. From this, and the definition of the X_2^*, it follows that $d - c - 1$ represents the number of bivariate observations, $(X_{1,j}, X_{2,j})$, that are located in the rectangular control region $C = \{(X_1, X_2): (L_1 < X_1 < M_1) \cap (L_2 < X_2 < M_2)\}$. We note that for the proposed control chart, the control limits for each component contribute to C, which is visualized below in Figure 1.

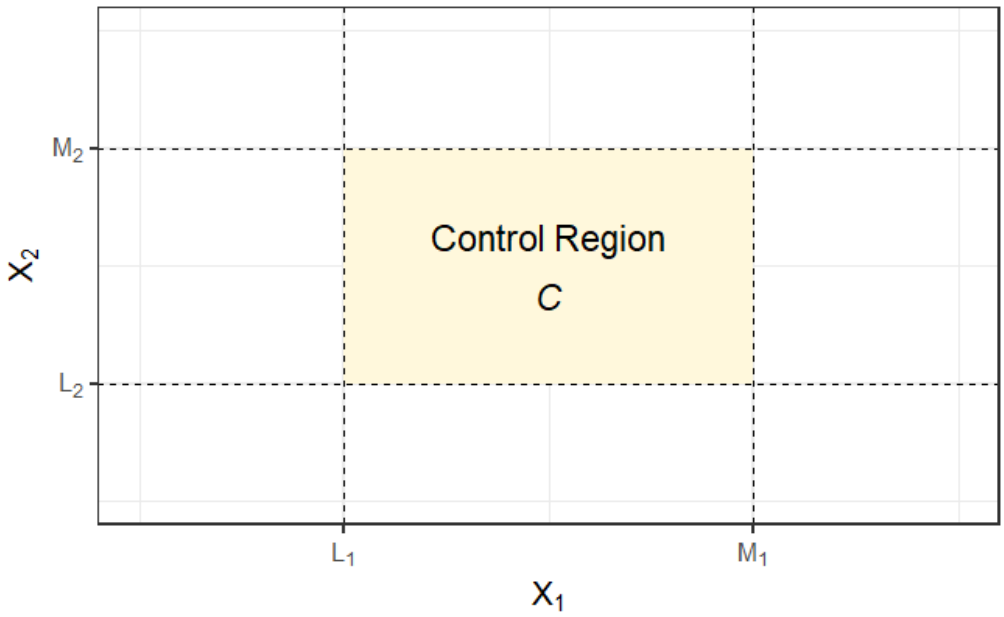

Figure 1: A graphical representation of the control region that defines the proposed bivariate control chart.

2.2 The Probability of a False Alarm

In the bivariate case, the event that an observation $\boldsymbol{X}$ from a Phase II sample falls in the control region, denoted $\boldsymbol{X} \in C$, is called a non-signalling event. As stated in Section 2.1, Q is the proportion of the bivariate universe included in C when the process is IC. Thus, Q is also the probability of the non-signaling event when the process is IC, that is, $Q = P(\boldsymbol{X} \in C|IC)$. From this, the probability of a false alarm (the false alarm rate) is given by $P = 1 - Q$.

Now, the event $\boldsymbol{X} \in C$ is equivalent to $\boldsymbol{X} \in (L_1 < X_1 < M_1) \cap (L_2 < X_2 < M_2)$ and therefore,

$$Q = \int_{L_2}^{M_2} \int_{L_1}^{M_1} f(x_1, x_2)\ dx_1 dx_2 \tag{2}$$

where $f(x_1, x_2)$ denotes the IC bivariate probability density function of (X_1, X_2). From the discussion in Section 2.1, and using Wald's result with our notation, we have that $Q \sim Beta(d - c, m - (d - c) + 1)$. Hence it can be shown that (see for example, Gibbons and Chakraborti, 2020, pp. 29-72) the probability of a false alarm, $P \sim Beta(m - (d - c) + 1, d - c)$. We now introduce a re-parameterization of the distribution of Q that depends on only m and a parameter k. This reduction of the number of parameters makes obtaining the control limits and calculating the chart performance much easier, and later the extension to the multivariate case smoother. To this end, letting $k = m - (d - c)$ and recalling the constraints from equation (1) on a, b, c, d, it follows that.

$$3 \leq k \leq m - 1 \tag{3}$$

Under this re-parameterization, $Q \sim Beta(m - k, k + 1)$ and thus $P = 1 - Q \sim Beta(k + 1, m - k)$. This key result will be used in section 2.3 to derive expressions for the run length distribution and various chart performance metrics of the proposed distribution-free control chart. Next, we discuss the IC run length distribution and then consider chart construction, that is how to find the values of the indices a, b, c, and d for the control limits, that satisfy some given performance measures based on the IC run length distribution. Among these measures, particular attention is given to ARL_0, which is a popular chart performance metric in the unknown parameter case.

In Section 2.1, we showed that $d - c - 1$ represents the number of Phase I observations such that $\boldsymbol{X} \in C$. So, it follows that $k = m - (d - c)$ represents one less than the number of Phase I observations such that $\boldsymbol{X} \notin C$. This relationship between k and the number of Phase I observations outside of the control region C may be noted for illustrative purposes.

2.3 IC Run Length Distribution

The IC run length $(\text{denoted } RL_0)$, corresponding to the number of plotted points on the control chart that fall inside the control region when the process is IC, before the first one falls outside (OOC signal), is a random variable. It is easy to see that the RL_0 distribution, given the order statistics that define the control region, that is, the conditional RL_0 distribution, follows a geometric distribution with success probability P. This result can be restated as the conditional RL_0 distribution given P, that is, $RL_0|P \sim Geometric(P)$, when the process is IC. Thus, RL_0 is a function of P, which is itself a random variable. Now, since the distribution of $P = 1 - Q$ is also known to be $Beta(k + 1, m - k)$ and does not depend on the underlying process distribution, we may use this information to derive the marginal distribution of RL_0 and, from this, the ARL_0 and the $Var(RL_0)$ in a distribution-free manner. See Appendix A for details and derivations. In addition to the marginal distribution of RL_0 being of interest, we are also interested in $E[RL_0|P]$, which is the so-called IC conditional average run length (denoted $CARL_0$). Note that $CARL_0 = \frac{1}{P}$ and thus is itself a random variable. Traditionally, the performance of a Phase II control chart is evaluated based on the unconditional (marginal) distribution of the IC run length, RL_0 and its various moments. This is the so-called unconditional perspective. However, chart performance has recently been evaluated based on the distribution of the $CARL_0$. This approach is called the conditional perspective (see, Jardim et al., 2020 for an in-depth discussion about the two perspectives) and is utilized to better account for the practitioner-to-practitioner variability which arises under estimated parameters. Following this literature, we consider chart construction according to both perspectives, and to this end we discuss both $CARL_0$ and RL_0, analytically deriving the respective distributions and calculating the expected values and variances, which serve as corresponding performance measures.

Since $CARL_0 = 1/P$ and P follows a beta distribution, in the bivariate case, the distribution of $CARL_0$ can be derived using the transformation of variables method, see Appendix B for details of this derivation and the derivation for the moments. Thus, the probability density function (PDF) and the cumulative distribution function (CDF) of $CARL_0$ are given by

$$f_{CARL_0}(r) = \frac{\Gamma(m+1)}{\Gamma(k+1)\Gamma(m-k)}\ r^{-(m+1)}(r-1)^{m-k-1}, \qquad r \geq 1, k < m \tag{4}$$

and

$$F_{CARL_0}(r) = 1 - \int_0^{\frac{1}{r}} \frac{\Gamma(m+1)}{\Gamma(k+1)\Gamma(m-k)}\ (t)^{k+1-1}(1-t)^{m-k-1}dt \tag{5}$$

respectively, with the IC mean and the variance given by

$$ARL_0 = E[CARL_0] = \frac{m}{k} \text{ and } \quad Var(CARL_0) = \frac{m(m-k)}{k^2(k-1)}, \tag{6}$$

respectively.

Finally, the distribution of RL_0 can be found by integrating the joint distribution of P, (the IC false alarm probability) and RL_0 over the range of P. Thus, in Appendix A it is shown that the IC probability mass function (PMF) and the CDF of RL_0 are given by

$$P(RL_0 = r) = \frac{m!\,(k+1)(m-k+r-2)!}{(m-k-1)!\,(m+r)!}, r = \{1,2,\dots\} \tag{7}$$

and

$$F_{RL_0}(r) = \begin{cases} 1 - \dfrac{m!\,(m-k+\lfloor r \rfloor - 1)!}{(m-k-1)!\,(m+\lfloor r \rfloor)!}, r \geq 1 \\ 0, \text{otherwise} \end{cases} \tag{8}$$

respectively, with the IC mean and the variances given by

$$ARL_0 = E[RL_0] = \frac{m}{k}, \qquad \text{and} \quad Var(RL_0) = \frac{m(k+1)(m-k)}{k^2(k-1)}, \tag{9}$$

respectively.

As is shown in Section 2.4, from these equations, the practitioner may find an appropriate value of k given some desired chart performance, commonly a desired (nominal) ARL_0 value, and from that one can find the indices a, b, c, and d that are needed for the construction of the control chart. Recall that k is defined as one less than the number of Phase I observations that do not fall in the control region C. Interestingly, note that it is shown and emphasized in Section 3.2 that given m and k, the equations (4)-(9) describe the IC probability distribution functions, the IC CDFs, and the moments for RL_0 and $CARL_0$ in the more general case of any multivariate continuous distribution, regardless of the dimension p.

2.4 Chart Construction: Determination of the Control Region in the Bivariate Case

In this section we discuss how to find the constants that determine the control limits for the bivariate chart. To this end, in order to determine the indices of the Phase I sample order statistics that serve as the control limits, we introduce two more constants, h and l such that equation (10) is satisfied:

$$\begin{aligned} h &= m - (b - a) + 1 \\ l &= m - h - (d - c) \\ h + l &= k \end{aligned} \tag{10}$$

From equation (10) and the discussion in Section 2.1, we may note that the constant h represents the number of Phase I observations such that the first component X_1 does not fall in the interval (L_1, M_1). Further, the constant l is one less than the number of observations from this subset such that the second component X_2 does not fall in the interval (L_2, M_2). From the inequalities in equations (1) and (3), it is clear that $h \geq 2$ and $l \geq 1$. Given that h is selected first, we have $h \leq -\max\{l\} - 1 = m - 2$ and $l \leq (m - 1) - h$. Thus, we are left with the following constraints:

$$\begin{aligned} 2 \leq h \leq m - 2 \\ 1 \leq l \leq m - h - 1 \end{aligned} \tag{11}$$

To find the values of the indices a, b, c, and d, the practitioner must first determine h and l. Thus, the first step is to determine or select the pair (m, k). If the Phase I sample size m is

given, the practitioner may solve for k as a function of m and ARL_0 using $ARL_0 = \frac{m}{k}$ given in equation (9). However, if the practitioner is in the position to select the Phase I sample size m, then any pair (m, k) may be chosen such that $3 \leq k \leq m - 1$ and $ARL_0 = \frac{m}{k}$. The selection process for (m, k) is explained in more detail in Section 2.6. After this, the practitioner must choose any h and l that satisfy equations (10) and (11). Recalling the constraints on a, b, c, d, in equation (1) we note that the possible values for (a, b) are

$$(1, m - h + 2), (2, m - h + 3), \dots, (h - 1, m) \tag{12}$$

and the possible values for (c, d) are:

$$(1, m - h - l + 1), (2, m - h - l + 2), \dots, (l, m - h) \tag{13}$$

Note that in the bivariate case, if $k = 3$, we get unique values $h = 2$ and $l = 1$, since $k = h + l$ and $h \geq 2$. This is true since $k = 3$ means that the control limits will be given by the minimum and the maximum for the first component and then for the new set in the second component the limits will also be the minimum and the maximum. This, in turn, yields unique values for $a, b, c,$ and d. However, when $k \geq 3$, the choice of the indices is not unique. In Section 2.3 we have shown that the distribution of RL_0 and $CARL_0$ depend only on k and m. Thus, the pairs (h, l) do not change the RL_0 or the $CARL_0$ distribution, as long as $k = h + l$ remains the same. Since all pairs (h, l) that satisfy equations (10) and (11) yield identical in-control chart performance, the choice is arbitrary. For simplicity, we suggest making h and $l + 1$ as equal as possible. Further, we recommend keeping the pairs of indices (a, b) and (c, d) obtained from (12) and (13), as "centered" as possible, meaning that we recommend selecting the "center" or the "middle" of the possible pairs. Thus, in the bivariate case, this means keeping the pair (a, b) as close to $\left(\frac{h}{2}, m + 1 - \frac{h}{2}\right)$ as possible and the pair (c, d) as close to $\left(\frac{l+1}{2}, m - h - \frac{l-1}{2}\right)$ as possible. In addition to simplicity, note that these choices also typically keep the IC tail probabilities for each component and between each component close to equal for both symmetric and skewed distributions, though the exact underlying process data distribution and the correlation among the variables may also affect the distribution of tail probabilities. Other

values for h and l and the indices may be considered if the practitioner is concerned about a specific OOC alternative. For an expanded discussion on this point, see Section 2 of the supplementary material.

Following this recommendation, if $k = 7$ and $m = 1400$, we choose $h = 4$ and $l = 3$. After this, we choose the middle pair of the possible pairs of $(a, b) = (2,1399)$, which are $(1, 1398)$, $(2, 1399)$, and $(3, 1400)$ from equation (12); and from (13) we choose the middle pair of the possible pairs of (c, d) which are $(1, 1394)$, $(2, 1395)$, and $(3, 1396)$. Note that $b - a - 1 = 1399 - 2 - 1 = 1396$. Thus the proposed control chart would be defined by the control region $\{(X_1, X_2): \left(X_{1,(2:1400)} < X_1 < X_{1,(1399:1400)}\right) \text{ and } \left(X^*_{2(2:1396)} < X_2 < X^*_{2(1396:1396)}\right)\}$ as in Section 2.1.

Next, we provide two brief examples for an illustration of these concepts. The first is a toy example that uses a real dataset to illustrate the construction of the control region. The second uses some simulated data to show how the control chart can be represented graphically.

2.5 Examples

In the first example, we illustrate the process of finding the control limits. Though the Phase I sample size will often be larger in practice, for illustrative purposes, assume that the following 25-observation dataset is the Phase I sample. This dataset, shown in Table 1, is well-known (Sultan, 1986; Chatterjee, 2019) and contains two quality characteristics: Brinell hardness and tensile strength. Let the Brinell hardness be denoted as X_1 and the tensile strength be as X_2. In this example, $m = 25$. Note that the ordering of the variables is arbitrary but reversing the order may result in a slightly different control region C. This difference is more pronounced in the toy example since the Phase I sample size is very small, but whenever the $ARL_0 \geq 27$, the difference is negligible and OOC performance is only very slightly affected. For a discussion on the ordering of the variables, see Section 2 of the supplementary material. Additionally, recall that theoretically, the permutation of the variable order does not impact the IC chart performance, since IC chart performance only depends on m and k. Continuing with the example, suppose that after choosing the desired value for ARL_0, it is determined that $k = 9$, from equation (9). From

this, the values h and l must be chosen from equations (10) and (11) such that $2 \leq h \leq 23, 1 \leq l \leq 24 - h$ and $h + l = 9$. Any values of h and l that satisfy these inequalities will maintain the same desired value for ARL_0. For this example, we will follow the recommendation from Section 2.4 and let $h = 4$ and $l = 5$. To begin, the Phase I sample must be sorted in ascending order in terms of X_1. Now, the pair (a, b) must satisfy equation (12). We will select $a = 2$ and $b = 24$, following the recommendation to "center" the indices. From this, we identify $L_1 = 143$ and $M_1 = 204$ as the lower and upper control limits for the X_1 component.

Table 1: Selection of control limits for Brinell hardness

	1	2	3	4	5	6	7	8	9	10	11	12	13
X_1	141	**143**	*148*	*160*	*161*	*162*	*168*	*172*	*175*	*177*	*178*	*178*	*179*
X_2	47.3	34.2	*47.8*	*45.5*	*48.4*	*45.9*	*47.5*	*49.4*	*57.3*	*50.6*	*51.5*	*50.9*	*51.2*

	14	15	16	17	18	19	20	21	22	23	24	25
X_1	*181*	*181*	*182*	*183*	*186*	*187*	*187*	*194*	*196*	*200*	**204**	215
X_2	*53.4*	*55.6*	*57.2*	*53.9*	*57.0*	*58.5*	*58.2*	*57.5*	*57.9*	*57.0*	55.1	59.1

Now that L_1 and M_1 have been identified, the focus is shifted to identifying L_2 and M_2. First, a subset is taken from the Phase I dataset. The 21 observations such that the Brinell hardness (X_1) falls between $L_1 = 143$ and $M_1 = 204$ (italicized in Table 1) are selected and rearranged in ascending order in terms of X_2, shown in Table 2. Given these sorted sets of observations, the pair (c, d) must satisfy equation (13). From this, we select $c = 3$ and $d = 19$, once again following the recommendation to "center" the indices. Thus, we identify $L_2 = 47.5$ and $M_2 = 57.9$ as the lower and upper control limits for the X_2 component.

Table 2: Selection of control limits for tensile strength

	1	2	3	4	5	6	7	8	9	10	11
X_1	160	162	168	*148*	*161*	*172*	*177*	*178*	*179*	*178*	*181*
X_2	45.5	45.9	**47.5**	*47.8*	*48.4*	*49.4*	*50.6*	*50.9*	*51.2*	*51.5*	*53.4*

	12	13	14	15	16	17	18	19	20	21
X_1	*183*	*181*	*186*	*200*	*182*	*175*	*194*	196	187	187
X_2	*53.9*	*55.6*	*57*	*57*	*57.2*	*57.3*	*57.5*	**57.9**	58.2	58.5

Thus, in this example, $L_1 = 143$, $M_1 = 204$, $L_2 = 47.5$, and $M_2 = 57.9$ define the Phase II bivariate control region for monitoring Brinell hardness and tensile strength. In other words, the Phase II control chart is defined by the control region $\{(X_1, X_2): (143 < X_1 < 204) \cap (47.5 < X_2 < 57.9)\}$. In this example, $ARL_0 = 2.78$. This ARL_0 value obviously is extremely low due to the small value for m in this example, illustrating that a much larger Phase I sample size will be required in practice for this chart. Detailed consideration for the Phase I sample size is discussed in Section 2.6 of the main text and Section 1 of the supplementary material.

For the second example, consider a simulated dataset with the Phase I sample size m to be 600. In this example, let $ARL_0 = 200$. Since m is given, k is determined uniquely as the solution to equation 7. Thus, $k = 3$. Further, since $k = 3$, the pair of values $h = 2$ and $l = 1$ are the unique solutions to the equations (10) and (11). Now, from equations (12) and (13), the values for a and b are found as 1 and 600 and the values for c and d are found as 1 and 598, respectively. These determine the control limits for the chart as $L_1 = X_{1,(1:600)}$ and $M_1 = X_{1,(600:600)}$ for the first component X_1 and $L_2 = X^*_{2,(1:598)}$ and $M_2 = X^*_{2,(598:598)}$ for the second component X_2. Note that X_2^* is defined as in Section 2.1. These limits define the rectangular control region.

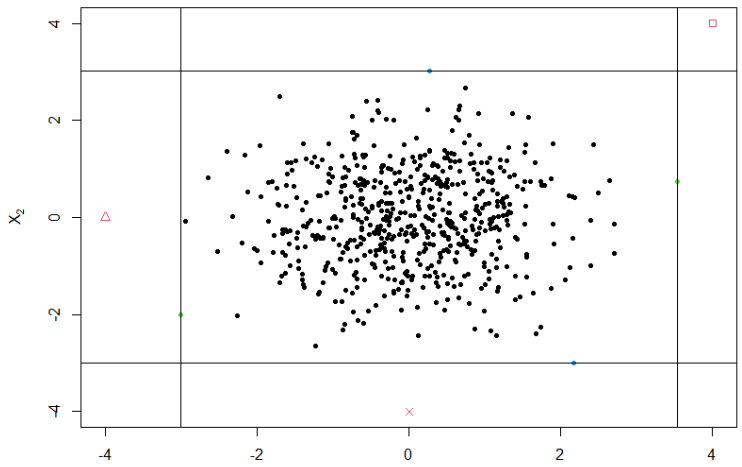

Figure 2: Simulated IC Phase I data from a bivariate normal distribution with mean vector 0 and covariance matrix equal to the identity. The vertical and horizontal lines are the control limits for X_1 and X_2, respectively. Three Phase II OOC points (in red) are added for illustration.

For this example, Figure 2 shows the 600 simulated observations from a bivariate normal distribution with $\boldsymbol{\mu} = (0, 0)^T$ and $\boldsymbol{\Sigma} = \boldsymbol{I}_2$ as the IC Phase I sample. The rectangular control region

is determined to be $\{(X_1, X_2)\colon (-3.01 < X_1 < 3.54) \cap (-3 < X_2 < 3.01)\}$ for the Phase II chart, using the values for a, b, c, d selected in the previous paragraph. Assume that at the 20th observation in Phase II, one of the following three observations is obtained:

1. (-4, 0), which is an OOC observation due to X_1 displayed by the symbol Δ,
2. (0, -4), which is an OOC observation due to X_2 displayed by the symbol ×, or
3. (4, 4), which is an OOC observation due to both X_1 and X_2 displayed by the symbol □.

Figure 3 shows how the OOC observations would appear in the proposed distribution-free Phase II control chart, which can be displayed as two univariate control charts jointly.

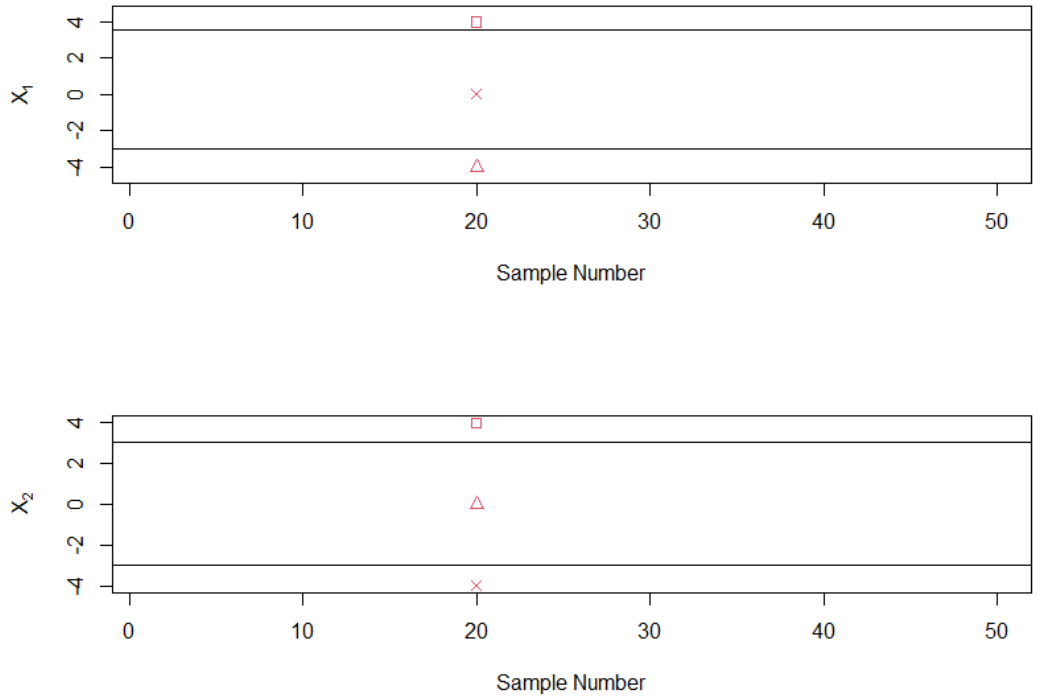

Figure 3: The proposed distribution-free control chart for a bivariate case showing three possible OOC observations in the 20th sample.

From Figure 2, it is easy to see that the values associated with the three hypothetical points are each outside of the control region. However, only □ is an outlier in terms of both components. Figure 3 presents this information during Phase II monitoring, allowing the practitioner to pinpoint which variables cause the signal. This is a practical advantage for the proposed chart. Note that the control chart in this example has the following IC performance: $ARL_0 = 200,\ SD(RL_0) = 282.13$, and $SD(CARL_0) = 141.07$.

Next, we consider chart performance measures and the issue of the necessary sample size for Phase I.

2.6 Performance Measures and Phase I Sample Size Considerations

One of the most commonly used chart performance measures in practice is the unconditional IC average run length, the $E[RL_0]$, denoted ARL_0, which is also equal to the expected value of the conditional IC average run length, $E[CARL_0]$. Since $\frac{m}{k} = ARL_0$ from equation (9), if m is given and $\frac{m}{ARL_0}$ is an integer, then k has a unique solution equal to $k = \frac{m}{ARL_0}$ such that $3 \leq k \leq m - 1$. As noted earlier, in some situations, the practitioner may be in the position to choose the Phase I sample size m. If this is the case, since $\frac{m}{k} = ARL_0$ is an equation with two unknowns, it has infinitely many solutions. A practitioner can find m for any given integer k. If the Phase I sample size m is chosen by the practitioner, then the construction of the proposed chart begins with selecting a pair (m, k). For example, if a practitioner desires a nominal $ARL_0 = 370$, then any pair (m, k) may be chosen such that m and k are integers, with $3 \leq k \leq m - 1$, and $\frac{m}{k} = 370$. Since several values of (m, k) satisfy this primary condition, some other condition, such as one involving $SD(RL_0)$ or $SD(CARL_0)$ may be used to choose a unique pair. For illustration, some pairs of values for (m, k) in this case are shown in Table 3.

Table 3: Some pairs (m, k) such that $ARL_0 = 370$, the corresponding $SD(RL_0)$, $SD(RL_0)/ARL_0$, $SD(CARL_0)$, and $SD(CARL_0)/ARL_0$ values

k	m	ARL_0	$SD(RL_0)$	$SD(RL_0)/ARL_0$	$SD(CARL_0)$	$SD(CARL_0)/ARL_0$
3	1,110	370	522.55	1.41	261.28	0.71
4	1,480	370	477.02	1.29	213.33	0.58
9	3,330	370	413.11	1.12	130.64	0.35
10	3,700	370	408.50	1.10	123.17	0.33
15	5,550	370	395.01	1.07	98.75	0.27
20	7,400	370	388.46	1.05	84.77	0.23
30	11,100	370	382.03	1.03	68.61	0.19
40	14,800	370	378.86	1.02	59.17	0.16
50	18,500	370	376.97	1.02	52.79	0.14

Though all pairs (m, k) in Table 3 yield ARL_0 values equal to the nominal 370, it may be observed that for a given ARL_0, the choice for the pair (m, k) affects the variability associated with IC run length distribution and hence the practitioner-to-practitioner variability. From Table 3, it may also be observed that as k increases, the Phase I sample size m increases by a factor of k but $SD(RL_0)$ and $SD(CARL_0)$, which are also used as chart performance measures, decrease. The $SD(RL_0)$ and $SD(CARL_0)$ are calculated as a function of m and k in equations (6) and (9). The standard deviation of the IC run-length or $SD(RL_0)$ measures the variability of RL_0 overall and $SD(CARL_0)$ measures the practitioner-to-practitioner variability.

In Section 1 of the supplementary material, we investigate the impact of the choice of the pair (m, k) on a variety of chart performance metrics. When a practitioner is in the position to choose the pair (m, k), we suggest using some value for the maximum of the ratio of $SD(CARL_0)$ to ARL_0, following the general framework of Zhang et al. (2014) and Saleh et al. (2015), to select a unique pair. In Section 1 of the supplementary material, we also consider using the exceedance probability criterion (EPC) (Jardim et al. 2020) as a primary chart performance metric for selecting a unique pair.

Next, we consider the general multivariate case.

3 The General Multivariate Case

3.1 The Setting

Wald (1943) extended his distribution-free bivariate TI to the general multivariate case with dimension p. Once again, this method constructs the tolerance region using m iid observations from a p-dimensional continuous distribution. Further, some indices, $r_1, s_1, r_2, s_2, \ldots, r_p, s_p$ are used to construct the p-dimensional tolerance region. Wald (1943) showed that $Q_p \sim Beta\left(s_p - r_p, m - \left(s_p - r_p\right) + 1\right)$, where Q_p denotes the probability content, regardless of the underlying data distribution. For the general multivariate case, we begin by detailing the construction of the tolerance region using Wald's method, which we use as a control region, and then introduce a reparameterization, akin to that in Section 2.2, allowing us to relate the IC signal probability, run length distribution, and conditional average run length distribution to that in the bivariate case.

Assume we have m multivariate observations from IC processes $(\boldsymbol{g}_1, \boldsymbol{g}_2, \dots, \boldsymbol{g}_m) = \Big(\big(X_{1,1}, \dots, X_{p,1}\big), \dots, \big(X_{1,m}, \dots, X_{p,m}\big)\Big)$. We would like to construct a control region $[L_1 \le X_1 \le M_1], [L_2 \le X_2 \le M_2], \dots, \big[L_p \le X_p \le M_p\big]$, with each L_i and M_i defined as order statistics as follows: Let $L_1 = X_{1,(r_1:m)}$ and $M_1 = X_{1,(s_1:m)}$ where, $r_1 < s_1 \le m$; then by considering only the remaining $s_1 - r_1 - 1$ points of X_2 where $X_{1(r_1:m)} < X_2 < X_{1(s_1:m)}$, denoted as X_2^*, choose $L_2 = X^*_{2,(r_2:s_1-r_1-1)}$ and $M_2 = X^*_{2,(s_2:s_1-r_1-1)}$. We continue by considering only the remaining $s_{i-1} - r_{i-1} - 1$ points of X_i where $X_{i-1,(r_{i-1}:m)} < X_1 < X_{i-1,(s_{i-1}:m)}$, denoted as X_i^*, choosing $L_i = X^*_{i,(r_i:s_{i-1}-r_{i-1}-1)}$ and $M_2 = X^*_{i,(s_i:s_{i-1}-r_{i-1}-1)}$, and repeating until we have $L_p = X^*_{p,(r_p:s_{p-1}-r_{p-1}-1)}$ and $M_p = X^*_{p,(s_p:s_{p-1}-r_{p-1}-1)}$.

This procedure is a generalization of the procedure proposed in Section 2.1 for the bivariate case. Note that in the bivariate case, the control limits for each component created a control region in the shape of a rectangle. In the more general multivariate case, the control limits create a control region in the shape of a hyperrectangle, denoted C_p.

3.2 The Probability of a False Alarm

Similar to the bivariate case, note that the probability content of C_p, denoted Q_p, is defined as in equation (14). This also denotes the probability of an IC non-signaling event, $\boldsymbol{X} \in C_p$, when p is the number of dimensions. Thus,

$$Q_p = \int_{L_p}^{M_p} \dots \int_{L_1}^{M_1} f\big(x_1, \dots, x_p\big)\, dx_1 \dots dx_p \tag{14}$$

where $f\big(x_1, \dots, x_p\big)$ denotes the IC joint p.d.f. of $(X_1, X_2, \dots, X_p)$. Using Wald's result, as in the bivariate case, we reparametrize the distribution such that it depends on only two parameters m and k instead of three parameters m s_p, and r_p. If we let $s_p - r_p = m - \sum_{i=1}^{p} d_i$ then

$$Q_p \sim Beta\Big(m - \sum_{i=1}^{p} d_i\,, \sum_{i=1}^{p} d_i\ + 1\Big)$$

where,

$$2 \leq d_1 \leq m - 2(p-1) \tag{15}$$

$$2 \leq d_j \leq m - 2(p-1-j) - \sum_{i=1}^{j-1} d_i \;\; \forall \;\; 1 < j < p \tag{16}$$

$$1 \leq d_p \leq m - 1 - \sum_{i=1}^{p-1} d_i \tag{17}$$

Now, we let $k = \sum_{i=1}^{p} d_i$. From equations (15) – (17), this implies

$$2p - 1 \leq k \leq m - 1 \tag{18}$$

We note that this restriction on k reduces to $3 \leq k \leq m-1$ when $p = 2$, as in Section 2.2. From the above, we observe that $Q_p \sim Beta(m-k, k+1)$. Further, we see from equations (15) – (17) that when $k = 2p - 1$, the choices for d_i are unique. Most importantly, we observe from the above that the distribution of Q_p is the same as the distribution of Q in the bivariate case shown in Section 2. Hence, the distribution of P_p, the false alarm probability, in the general multivariate case, is also only a function of m and k and is distributed as P in the bivariate case. Thus, equations (4) – (9) hold for the multivariate chart regardless of dimension p. So, the distributions of RL_0 and $CARL_0$ and the associated moments are functions of only m and k and not a function of p. Thus, the relationships between (m, k) and ARL_0, $SDRL_0$, $SDCARL_0$, and $P(CARL_0 > a)$ established in the bivariate case also hold for the multivariate case in general.

Next, we consider the chart construction in the general multivariate case.

3.3 Chart Construction: Determination of the Control Region in the General Multivariate Case

To find the values of $r_1, s_1, r_2, s_2, \ldots, r_p$, and s_p, the practitioner must first determine the value of k. As before, if the practitioner is in the position to choose the Phase I sample size m, then he/she must choose a pair of values (m, k). The pair (m, k) may be chosen to satisfy some desired performance metric such as ARL_0 or $P(CARL_0 > r) = \gamma$. The consideration given for this choice in the bivariate case (Section 2.6) is applicable here, with the only difference being the more general restriction $k \geq 2p - 1$. Then, the practitioner must choose the d_i's such that

(15)-(17) are satisfied and $\sum_{i=1}^{p} d_i = k$. These values d_i are analogous to h and l in the bivariate case. Finally, the possible values for (r_1, s_1) are

$$(1, m - d_1 + 2), (2, m - d_1 + 3), \dots, (d_1 - 1, m), \tag{19}$$

and the possible values for (r_j, s_j) for $1 < j < p$ are

$$\left(1, m - \left(\sum_{i=1}^{j} d_i\right) + 2\right), \left(2, m - \left(\sum_{i=1}^{j} d_i\right) + 3\right), \dots, \left(d_j - 1, m - \left(\sum_{i=1}^{j-1} d_i\right)\right) \tag{20}$$

for all $1 < j < p$ and the possible values for (r_p, s_p) are:

$$(1, m - k + 1), (2, m - k + 2), \dots, \left(d_p, m - k + d_p\right) \tag{21}$$

As noted above, whenever $k = 2p - 1$, the choices for d_i are unique such that $d_i = 2$ for $i < p$ and $d_p = 1$. In this case, equations (19) – (21) yield unique choices for all (r_i, s_i) pairs. To understand the meaning of these values, we note that d_1 is the number of Phase I observations such that the first component X_1 does not fall in the interval $\left(X_{1,(r_1)}, X_{1,(s_1)}\right)$. Further, $\sum_{i=1}^{n} d_i$ for $n = \{2, \dots, p\}$ is the number of Phase I observations such that for at least one $j \leq n$ the $j - th$ component X_j does not fall in the interval $\left(X_{1,(r_j)}, X_{1,(s_j)}\right)$.

For example, let $p = 3$ and the desired $ARL_0 = 200$. We first note that from equation (21), $k \geq 5$. Using the minimum k, we identify the pair $(k = 5, m = 1000)$ as satisfying equation (9). Since d_1 and d_2 would have to be at least 2 and $\sum_{i=1}^{p} d_i = k$, we choose $d_1 = 2$, $d_2 = 2$, and $d_3 = 1$ as the unique selections. From equations (19) – (21), the values for r_1 and s_1 are 1 and 1000, the values for r_2 and s_2 are 1 and 998, and the values for r_3 and s_3 are 1 and 996. In general, we follow the same rule of thumb in making the d_i's as equal as possible for simplicity and for desirable chart properties. We also advise selecting the pair of indices from (19) – (21) as "centered" as possible, meaning that the middle possible pair should be chosen. For further motivation of this selection, see Section 2 of the supplementary material. Following the recommendation leads to choosing pairs equal or close to the following:

$$(r_1, s_1) = \left(\frac{d_1}{2}, m + 2 - \frac{d_1}{2}\right);$$

$$\left(r_j, s_j\right) = \left(\frac{d_j}{2}, m + 2 - \sum_{i=1}^{j-1} d_i - \frac{d_j}{2}\right) \text{ for } 1 < j < p;$$

and

$$\left(r_p, s_p\right) = \left(\frac{d_p+1}{2}, m - k + \frac{d_p+1}{2}\right).$$

The construction of the control region in the multivariate case is analogous to the construction in the bivariate case and is easily applied for any $p \geq 2$. Further, following the equations throughout Section 3, setting up the chart is straightforward given some desired chart performance metric. The flowchart in Figure 4 presents this same information in an algorithmic manner to assist the practitioner.

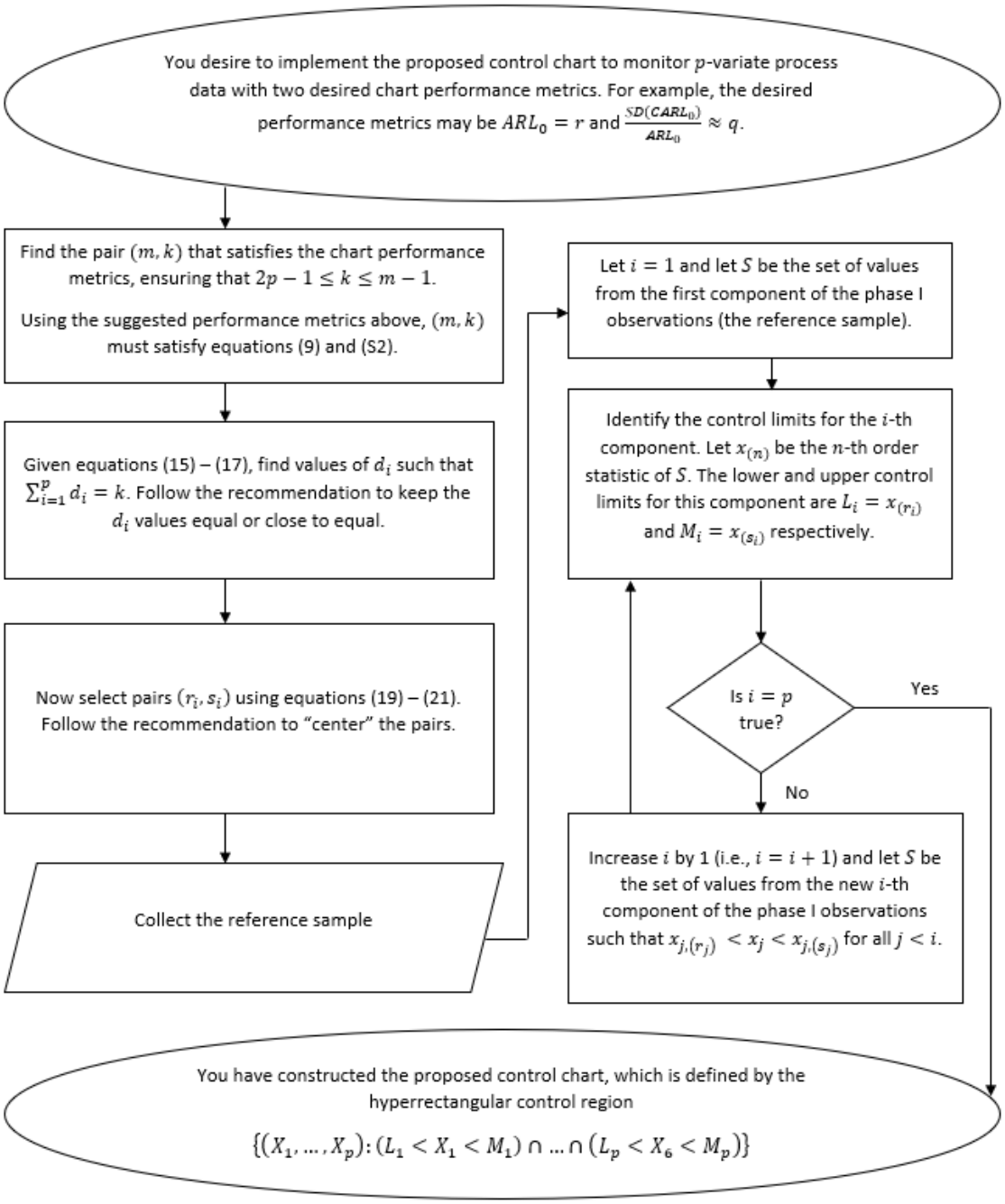

Figure 4: A Flowchart for use in constructing the chart

4 Out of Control Chart Performance

An investigation about the performance of the chart in the OOC case is important. Since exact calculations are complicated (for example, OOC performance is not distribution-free), we resort to simulation studies to evaluate OOC performance for the proposed method and for a popular competitor, the Hotelling's T^2 chart. We choose the T^2 chart since we believe that practitioners considering our method will find themselves choosing between these two charts. As for other charts, to the best of our knowledge, no Case U multivariate control chart exists in the literature that is exactly distribution-free, easy to implement with simple post signal diagnostics, and does not require a prohibitively large reference sample size. Thus, we now turn to the particular alternatives under which the proposed method and the Hotelling's T^2 chart will be evaluated. The OOC performance of the proposed control chart is considered for $ARL_0 = 200$ and $p = \{2, 6, 10\}$. The following IC distributions for the IC Phase I sample are considered: (i) multivariate normal with mean vector 0, denoted as N_p; (ii) heavier-tailed multivariate t with ξ degrees of freedom, denoted as $t_{p,\xi}$; (iii) skewed multivariate gamma, where the marginal univariate gamma distributions associated with each component have shape parameter ζ and rate parameter $\sqrt{\zeta}$, denoted as $\mathrm{Gam}_{p,\zeta}$. For each distribution, the covariance matrix $\Sigma = (\sigma_{ij})$ is chosen to be $\sigma_{ij} = 0.5^{|i-j|}$, for $i, j = 1, 2, \ldots, p$. A location shift of size $\delta = \{1, 2, 4\}$ in the first $[p/2]$ components is used in the OOC case, i.e., $\boldsymbol{X_i} + \delta \mathbf{e}_1$ where $\mathbf{e}_1 = \left(\underbrace{1, \ldots, 1}_{1, \ldots, p/2}, 0, \ldots, 0\right)^T$. Since the chart is designed to monitor a change in location, we do not include a change in dispersion when considering the OOC cases for the multivariate normal or multivariate t distributions. However, for the multivariate gamma distribution, the location and scale both depend on ζ, so the OOC case includes a location and scale change. All the results in this section are obtained from 10,000 replications.

For the control chart to have an $ARL_0 = 200$, k must satisfy equation (18) and the pair (m, k) must satisfy equation (9). Thus, we consider three scenarios for (m, k):

(i) $m = 200(2p - 1), k = 2p - 1$

(ii) $m = 200(5)(2p - 1), k = 5(2p - 1)$

(iii) $m = 200(10)(2p-1), k = 10(2p-1)$

Tables 4, 5, and 6 demonstrate the OOC performance of the proposed chart and the Hotelling's T^2 chart under these conditions (Montgomery, 2020). The results for the proposed chart are shown above, with the Hotelling's T^2 results following immediately under, for a comparison under each distribution. In Table 4, the underlying distribution is multivariate normal; in Table 5, the underlying distribution is multivariate t; and in Table 6, the underlying distribution is multivariate gamma. The Hotelling's T^2 chart is chosen since it is among the most widely used, well known, and easy to construct, included in a number of software packages.

It should be noted that since the Hotelling's T^2 control chart is a parametric chart under the normality assumption and the proposed chart is distribution-free, the proposed chart is expected to perform comparatively better when the normality assumption is violated. Thus, we have utilized a Monte-Carlo adjustment to ensure that that the Hotelling's T^2 chart maintains the nominal ARL_0 value under each OOC scenario. We note that this is not a completely fair comparison since this adjustment requires the knowelege of the underlying distribution while the proposed method does not. Nonetheless, we present this comparison to show how the proposed method performs against the popular Hotelling's T^2 chart when the practitioner knows the underlying process distribution.

Table 4: The OOC performance for the proposed distribution-free control chart and the Hotelling's T^2 control chart when the IC Phase I sample is generated from N_p distribution for different values of p, m, and δ.

			$\delta = 0$		$\delta = 1$		$\delta = 2$		$\delta = 4$	
	p	m	ARL	$SDRL$	ARL	$SDRL$	ARL	$SDRL$	ARL	$SDRL$
Proposed Chart	2	600	197.86	263.99	63.26	122.12	9.54	18.74	1.26	0.65
		3000	197.84	209.66	45.38	51.06	6.90	6.93	1.21	0.51
		6000	201.24	202.44	44.44	46.39	6.61	6.36	1.20	0.49
	6	2200	198.37	213.71	41.32	48.27	5.42	5.49	1.08	0.30
		11000	195.59	196.97	35.22	35.37	4.88	4.40	1.07	0.27
		22000	199.27	201.10	35.59	35.83	4.75	4.34	1.07	0.27
	10	3800	198.33	208.09	34.83	38.35	4.49	4.14	1.04	0.20
		19000	200.21	204.41	31.72	31.17	4.13	3.65	1.03	0.18
		38000	202.24	203.80	31.66	31.40	4.08	3.55	1.03	0.17
T^2 Chart	2	600	196.74	201.84	29.80	30.57	4.47	4.02	1.07	0.27
		3000	200.46	203.05	30.15	30.26	4.51	4.03	1.07	0.28
		6000	202.54	201.19	31.37	30.80	4.55	4.05	1.08	0.30
	6	2200	200.43	198.29	37.97	37.90	4.55	4.06	1.03	0.19
		11000	202.82	202.70	37.52	37.01	4.53	4.03	1.03	0.18
		22000	190.50	192.71	36.12	35.86	4.39	3.82	1.03	0.18
	10	3800	199.42	200.43	36.79	36.35	3.90	3.39	1.01	0.11
		19000	197.40	195.29	35.99	36.17	3.79	3.22	1.01	0.11
		38000	199.61	201.67	36.56	36.54	3.85	3.35	1.01	0.11

Table 5: The OOC performance for the proposed distribution-free control chart and the Monte-Carlo adjusted Hotelling's T^2 control chart when the IC Phase I sample is generated from $t_{p,5}$ distribution for different values of p, m, and δ.

			$\delta = 0$		$\delta = 1$		$\delta = 2$		$\delta = 4$	
	p	m	ARL	$SDRL$	ARL	$SDRL$	ARL	$SDRL$	ARL	$SDRL$
Proposed Chart	2	600	200.42	287.78	177.73	271.14	135.14	244.95	54.66	177.01
		3000	204.69	218.97	176.66	196.05	109.78	135.69	19.21	38.27
		6000	201.10	204.91	167.88	172.63	102.76	116.09	15.05	22.01
	6	2200	203.46	224.43	174.25	194.89	125.93	157.80	32.48	68.36
		11000	200.12	204.01	176.07	180.38	120.88	127.56	23.51	28.47
		22000	200.26	201.85	174.03	177.84	118.25	122.45	22.71	24.52
	10	3800	199.06	206.66	178.37	189.83	126.85	145.52	30.80	49.49
		19000	204.52	207.67	180.43	182.10	126.56	132.04	28.45	30.20
		38000	199.48	200.73	182.06	186.42	128.01	130.65	29.16	30.26
T^2 Chart	2	600	199.26	206.56	157.96	161.64	80.82	85.06	8.28	9.31
		3000	198.92	197.93	157.68	158.05	78.32	78.40	7.91	7.83
		6000	202.12	203.56	158.00	159.19	79.72	79.16	7.79	7.40
	6	2200	201.88	200.86	180.97	181.89	138.80	138.63	37.80	38.23
		11000	201.02	201.66	185.85	185.44	138.62	137.85	36.58	36.20
		22000	200.82	205.52	180.06	178.50	135.28	134.49	36.82	36.90
	10	3800	207.20	206.57	192.18	193.87	155.52	158.55	60.42	60.80
		19000	201.00	198.15	186.14	187.10	148.60	149.40	57.74	56.85
		38000	200.78	196.63	187.45	186.31	154.35	153.24	59.55	59.53

Table 6: The OOC performance for the proposed distribution-free control chart and the Monte-Carlo adjusted Hotelling's T^2 control chart when the IC Phase I sample is generated from $\mathrm{Gam}_{p,3}$ distribution for different values of p, m, and δ.

			$\delta = 0$		$\delta = 1$		$\delta = 2$		$\delta = 4$	
	p	m	ARL	$SDRL$	ARL	$SDRL$	ARL	$SDRL$	ARL	$SDRL$
Proposed Chart	2	600	200.94	279.28	166.23	268.45	73.32	139.18	12.37	77.57
		3000	200.72	214.98	137.66	148.27	50.95	62.64	4.86	5.57
		6000	199.82	204.36	137.16	144.74	47.98	51.14	4.60	4.62
	6	2200	202.28	224.84	141.23	169.07	52.34	64.99	5.23	6.70
		11000	200.56	200.55	133.78	140.84	45.16	46.93	4.46	4.16
		22000	204.64	206.82	132.61	134.17	43.76	44.72	4.41	3.92
	10	3800	201.06	210.92	137.95	152.59	47.50	55.20	4.64	4.84
		19000	197.03	200.14	130.68	132.37	42.92	43.22	4.23	3.79
		38000	203.54	201.49	129.20	129.66	42.30	43.16	4.23	3.74
T^2 Chart	2	600	202.31	212.18	77.75	82.60	20.50	21.05	1.81	1.31
		3000	202.38	203.51	75.60	76.00	20.28	19.70	1.75	1.16
		6000	201.25	200.94	76.57	75.95	20.40	20.39	1.73	1.14
	6	2200	200.94	201.74	87.60	88.62	24.19	24.03	1.80	1.22
		11000	199.35	201.02	87.26	87.87	23.63	22.80	1.77	1.16
		22000	196.86	197.19	84.19	83.45	23.21	22.40	1.77	1.16
	10	3800	200.95	200.71	83.57	84.82	21.08	20.34	1.44	0.80
		19000	202.74	202.83	82.49	81.67	21.08	20.70	1.46	0.81
		38000	202.66	201.09	85.25	85.53	20.83	20.42	1.46	0.81

In Tables 4, 5, and 6, we see that as δ increases the OOC ARL and $SDRL$ decrease considerably for the proposed control chart and the Hotelling's T^2 chart. The change in the OOC ARL and $SDRL$ for the proposed method is of a different magnitude depending on the distribution which is not surprising since the OOC performance is not distribution-free. However, the proposed control chart appears to be effective at detecting location shifts with a variety of distributions of different shapes.

As one might expect when the process data follows the multivariate normal distribution, the Hotelling's T^2 chart performs comparitively better than the proposed chart. With the two charts set to achieve the same ARL_0, the Hotelling's T^2 chart typically experiences slightly smaller $SDRL_0$ values. Under each OOC scenario, the proposed chart tends to fail at detecting the shift as quickly, also experiencing larger $SDRL$ values. Despite this, the difference in chart

performance is very slight when $\delta = 2$ and is negligible when $\delta = 4$. This is largely the same when the underlying distribution is $\mathrm{Gam}_{p,3}$.

However, the narritive changes considerably when the underlying process distribution is $t_{p,5}$. Here, the performance is similar in many cases. As the dimmensionality increases to $p = 6$ or $p = 10$, the proposed method tends to detect the shift more quickly. From this, it may seem that the proposed method experiences only a marginal advantage over the Hotelling's T^2 chart in some cases. However, this is far from true. In practice, it is much more likely that the underlying process distribution is unknown. While the proposed method maintains the same IC performance regardless of the underlying distribution, the Hotelling's T^2 chart is not IC robust. For example, see Table 7.

Table 7: The true IC performance the Hotelling's T^2 control chart when the underlying distribution is unknown and the Normal UCL is utilized. Results from 10,000 replications.

p		2			6			10		
m		600	3000	6000	2200	11000	22000	3800	19000	38000
$t_{p,5}$	ARL_0	43.18	43.98	44.61	21.33	21.34	21.79	15.61	15.74	15.87
	$SDRL_0$	43.43	44.02	43.91	21.12	21.02	21.93	15.06	15.35	15.50
$\mathrm{Gam}_{p,3}$	ARL_0	45.13	45.56	45.51	28.25	28.75	27.62	24.68	24.04	24.34
	$SDRL_0$	45.51	45.80	44.65	28.18	28.42	27.51	23.84	23.49	23.73

The Hotelling's T^2 chart suffers from drastically smaller achieved ARL_0 values compared to the nominal values when the process distribution is unknown. This is true for both the $t_{p,5}$ and $\mathrm{Gam}_{p,3}$ distributions. The problem is amplified when the dimension is larger. In Table 7, when $p = 10$, the Hotelling's T^2 chart yields a true ARL_0 values less than 25 when the distribution is $t_{p,5}$ and ARL_0 values less than 14 when the distribution is $\mathrm{Gam}_{p,3}$. Thus, the chart performance is undesirable in these conditions due to the small ARL_0. We conclude this OOC performance comparison by noting that by using the proposed method instead of the Hotelling's T^2 chart, the practitioner sacrifices very little when the underlying distribution is known and yet experiences a significant advantage when the underlying distribution is unknown. Thus, the proposed distribution-free chart seems to be preferable whenever the distribution of the process data is not known with certainty and is possibly heavy-tailed or skewed.

5 Illustrative Examples

5.1 Multivariate Board Thickness Example

In order to illustrate the practical applications of the proposed method, next we consider monitoring board thickness measurements in the multivariate case. For each board, six measurements were taken to measure thickness at six different positions (Dunn, 2018). For illustration, we use the first 2200 boards as the reference (Phase I) sample, assuming that these board thickness measurements follow the in-control distribution. We use these data to set up a control chart such that $ARL_0 = 200$ to monitor the next 100 boards. From an exploratory analysis, the data appear to be non-normal. To this end, note that a Henze-Zirkler (Henze and Zirkler, 1990) test for multivariate normality yields a p-value < 0.001 and a Shapiro-Wilks test for each component yield p-values < 0.001, also challenging the multivariate normal assumption. Additionally, the sample correlation values between the components range from 0.12 to 0.62. Data such as these emphasize the benefit of a distribution-free method, such as the proposed chart.

Table 8: Lower and upper control limits for the six-variate board thickness phase II chart

i	r_i	L_i	s_i	M_i
1	1	1329	2200	1862
2	1	1427	2198	1811
3	1	1278	2196	1817
4	1	1381	2194	1845
5	1	1311	2192	1804
6	1	1377	2190	1825

In choosing the chart constants, we find that $k = 11$ satisfies the equation for $\frac{m}{k} = ARL_0$. To satisfy equations (15) – (18), we find $d_i = 2$ for $i = 1, 2, 3, 4, 5$, and $d_6 = 1$. Now, the pairs (r_i, s_i) are found according to equations (19) – (21), yielding the lower and upper limits L_i and M_i for the $i - th$ component. Ties in the dataset are broken randomly. These values are listed in Table 8. These control limits define the Phase II multivariate control chart such that the control

region is the hyperrectangle $\{(X_1, X_2, X_3, X_4, X_5, X_6): (L_1 < X_1 < M_1) \cap (L_2 < X_2 < M_2) \cap \ldots \cap (L_6 < X_6 < M_6)\}$. As in the bivariate board example, we have $ARL_0 = 200$, $SDRL_0 = 218.54$, and $SD(CARL_0) = 63.09$. Despite the difference in dimension p, the IC chart performance is identical since it depends only on m and k.

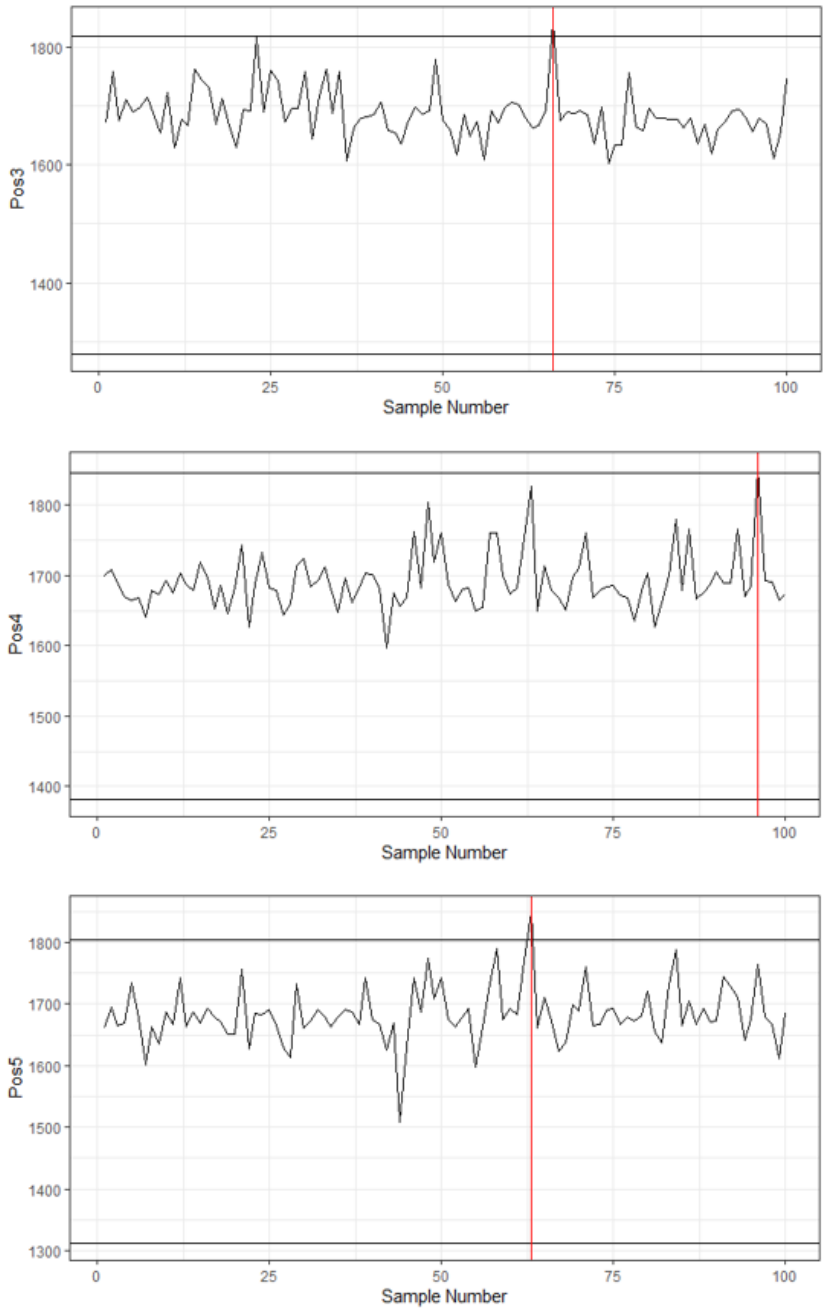

Figure 5: The proposed control chart for the six-variate board thickness phase II data as applied to the third, fourth, and fifth components. Red lines indicate that the component lead to the signal.

Monitoring the 100 Phase II observations, the chart signals at observations 63, 66, and 96. As highlighted before, it is not always easy to pinpoint the variable that causes a signal in multivariate process monitoring with many of the available charts in the literature. However, the proposed chart allows us to see that the spikes in components 3, 4, and 5 lead to the alarms. This makes a post signal diagnostic more convenient and efficient. Figure 5 allows us to visualize the monitoring scheme as it relates to each component. A red line has been added in each plot to indicate that the component has caused a signal.

5.2 Simulated Data Example

Finally, we use a simulated multivariate data set, $p = 3$, to illustrate the construction of the proposed control chart. A simulated example is chosen to contrast with the real data example in 5.1. Since the data are simulated, we are able to introduce a shift and see if the chart is able to detect the shift and signal. Now to the construction of the chart, the desired performance metrics are $ARL_0 = 200$ and $SD(CARL_0)/ARL_0 < 0.5$. Given the restriction $2p - 1 = 5 \leq k \leq m - 1$, we note that the smallest values for k and m that satisfy these metrics yield the pair $(k = 5, m = 1000)$, by equation (6). The data set is obtained as follows. Let $\boldsymbol{g}$ follows an IC distribution N_3 with $\boldsymbol{\mu} = (0, 1, 2)^T$ and $\Sigma = \Sigma_1 = (\sigma_{ij})$ is chosen to be $\sigma_{ij} = 0.5^{|i-j|}$, for $i, j = 1, 2, 3$. We generate 1000 sample points as a Phase I sample shown in Figure 6. Let $\boldsymbol{G} = (\boldsymbol{g}_1, \dots, \boldsymbol{g}_{1000})^T = (X_1, X_2, X_3)$. We also generate 80 sample points as a Phase II sample, in Appendix C (Table 9), where the first 40 sample points are generated from the IC distribution and the last 40 are generated from N_3 with $\boldsymbol{\mu} = (4, 1, 2)^T$ and $\Sigma = \Sigma_1$. Note that there is a clear mean shift in X_1 for the last 40 Phase II data points. In principle, we should expect the chart to detect this change. As Figure 7 shows, this is indeed the case.

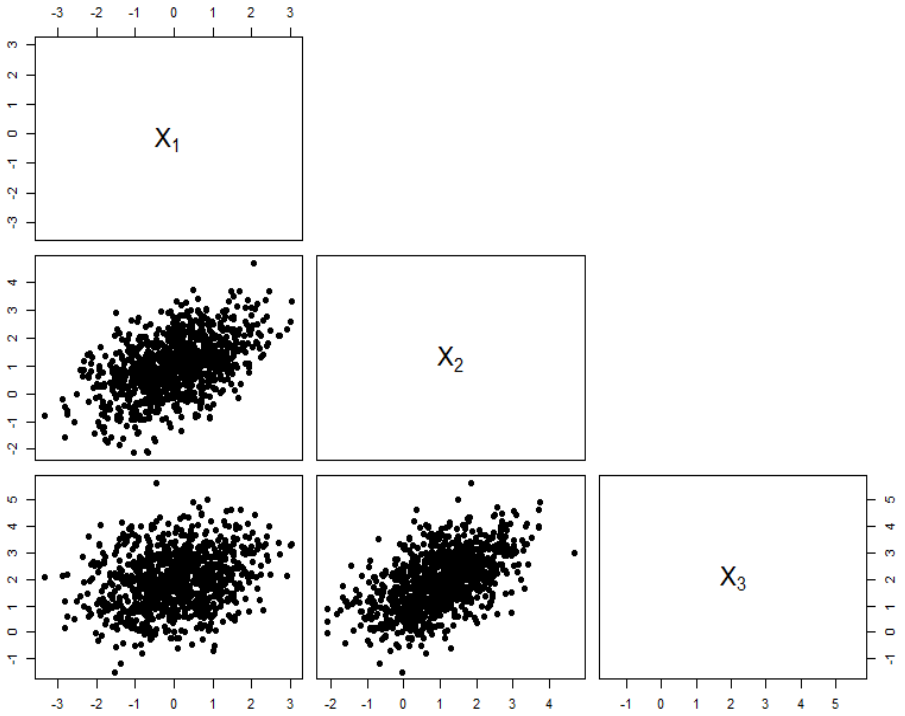

Figure 6: The simulated IC phase I sample.

Since d_1 and d_2 must be at least 2 and $\sum_{i=1}^{3} d_i = k$, we choose $d_1 = 2$, $d_2 = 2$, and $d_3 = 1$. The values for r_1 and s_1 are 1 and 1000, the values for r_2 and s_2 are 1 and 998, and the values for r_3 and s_3 are 1 and 996. The control region for the proposed control chart is the hyperrectangle defined by $\{(X_1, X_2, X_3): (L_1 < X_1 < M_1) \cap (L_2 < X_2 < M_2) \cap (L_3 < X_3 < M_3)\}$. In this construction, we have $L_1 = X_{1,(1:1000)}$ and $M_1 = X_{1,(1000:1000)}$; then considering only the remaining 998 points where $X_{1,(1:1000)} < X_1 < X_{1,(1000:1000)}$ we have $L_2 = X^*_{2,(1:998)}$ and $M_2 = X^*_{2,(998:998)}$; then considering only the remaining 996 points where $X^*_{2,(1:998)} < X_2 < X^*_{2,(998:998)}$ we have $L_3 = X^*_{3,(1:996)}$ and $M_3 = X^*_{3,(996:996)}$. From our simulated data, the hyperrectangular control region for the proposed control chart is defined by $(-3.34 < X_1 < 3.04)$ and $(-2.10 < X_2 < 4.67)$ and $(-1.49 < X_3 < 5.61)$.

The construction and implementation of the proposed chart is easy in the sense that it can be presented (visualized) as three univariate control charts where the limits are calculated at the multivariate level. Finding the order statistic as demonstrated previously is relatively easy.

From Figure 7, we can see that the charts are on the original scale and we are able to pinpoint the variable causing the OOC signal.

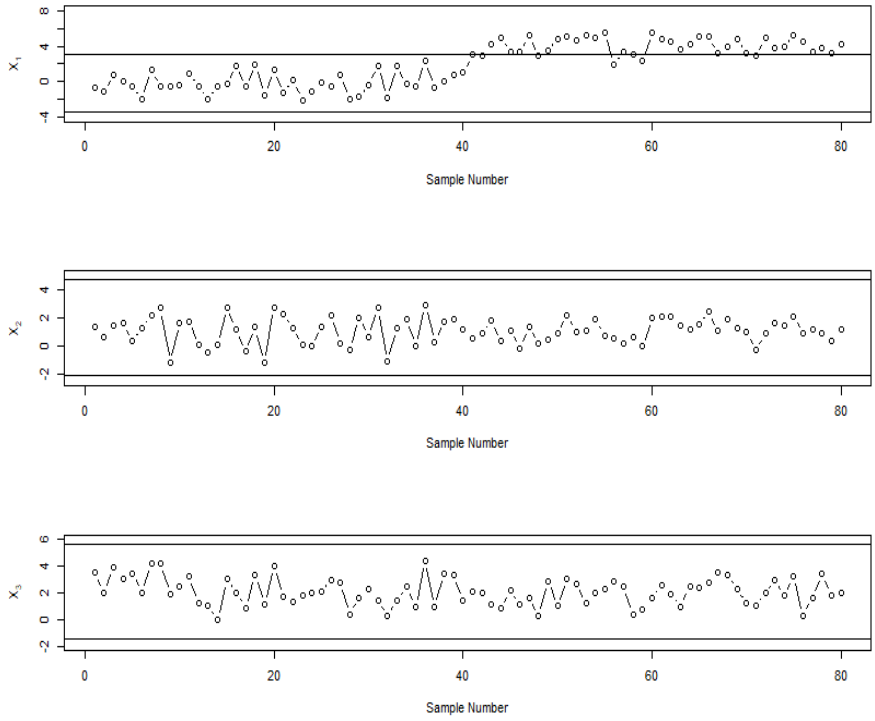

Figure 7: Proposed control chart for the simulated phase II sample for the data in Appendix B

6 Summary and Conclusions

In this paper, we extend a univariate distribution-free Phase II Shewhart-type control chart based on Phase I order statistics to the multivariate case by adopting an existing distribution-free multivariate tolerance interval. The proposed multivariate distribution-free control chart can be visualized as p univariate Shewhart-type control charts where the limits are obtained jointly for a nominal ARL_0 value. This allows the chart to maintain a specified ARL_0 and pinpoint the variables that cause an OOC signal, which leads to an implementation strategy allowing for simple post signal diagnostics, an important practical advantage. The IC performance is expressible in a closed form under the unconditional and the conditional perspectives. One major requirement is a large Phase I sample. The need for the large Phase I sample size is to reduce the practitioner-to-practitioner variation and to allow the practitioner to construct the chart to achieve some typically desired IC performance. In addition, higher dimensional

monitoring requires relatively larger Phase I sample sizes. However, in the modern monitoring environment, this may not be a very restrictive condition. A simulation study of the OOC performance is presented and shows that the proposed distribution-free chart is able to detect a number of shifts and is competitive against the normal theory based Hotelling's T^2 chart in some situations. Multiple illustrations for the implementation of the control chart, using real and simulated data, are provided.

To summarize, the proposed method fills a gap in the literature. There are currently no Case U multivariate control charts in the literature that are exactly distribution-free, simple for practitioners to use (included in software packages, with provided codes, or straightforward instructions) with a clear/automatic post signal diagnostic, and do not require a prohibitively large reference sample size. The proposed control chart is thus recommended, which is simple to construct and interpret, is exactly distribution-free, generalizes a well-known univariate distribution-free control chart, requires no complex parameter estimation calculations to implement, comes with immediate post signal diagnostics, and only requires a modestly large reference sample size for small to moderate p.

Acknowledgements

The authors would like to thank the two anonymous reviewers for their comments that have improved the paper.

References

Bersimis, S., Psarakis, S., & Panaretos, J. (2007). *Multivariate statistical process control charts: an overview.* Quality and Reliability engineering international, 23(5), 517-543.

Bersimis, S., Sgora, A., & Psarakis, S. (2017). *Methods for interpreting the out-of-control signal of multivariate control charts: A comparison study*. Quality and Reliability Engineering International, 33(8), 2295-2326.

Chakraborti, S. (2014). Nonparametric (distribution-free) quality control charts. Wiley StatsRef: Statistics Reference Online.

Chakraborti, S., & Graham, M. (2019). *Nonparametric Statistical Process Control.* Wiley.

Chakraborti, S., & Graham, M. A. (2019). Nonparametric (distribution-free) control charts: An updated overview and some results. *Quality Engineering, 31*(4), 523-544.

Chakraborti, S., Human, S. W., & Graham, M. A. (2008). Phase I statistical process control charts: An overview and some results. *Quality Engineering*, 21(1), 52-62.

Chakraborti, S., Qiu, P., & Mukherjee, A. (2015). Editorial to the special issue: Nonparametric statistical process control charts. *Quality and Reliability Engineering International*, *31*(1), 1-2.

Chakraborti, S., Van der Laan, P., & Van de Wiel, M. (2004). A Class of Distribution-Free Control Charts. *Journal of the Royal Statistical Society. Series C (Applied Statistics), 53*(3), 443-462.

Chatterjee, M. (2019). Impact of multivariate normality assumption on multivariate process capability indices. *Communications in Statistics: Case Studies, Data Analysis and Applications*, *5*(4), 314-345.

Dunn, K. (2018) *Six-point board thickness* [csv file]. https://openmv.net/info/six-point-board-thickness

Gibbons, J. D., & Chakraborti, S. (2020). *Nonparametric statistical inference*. CRC press.

Ge, Z., & Song, Z. (2013). *Multivariate Statistical Process Control : Process Monitoring Methods and Applications.* London: Springer.

Hamada, M. (2002). *Bayesian tolerance interval control limits for attributes*. Quality and Reliability Engineering International, 18(1), 45-52.

Hamada, M. (2003). *Tolerance interval control limits for X, R, and S charts*. Quality Engineering, 15(3), 471-487.

Henze, N., & Zirkler, B. (1990). A class of invariant consistent tests for multivariate normaility. *Communications in statistics-Theory and Methods*, *19*(10), 3595-3617.

Jardim, F. S., Chakraborti, S., & Epprecht, E. K. (2020). Two perspectives for designing a phase II control chart with estimated parameters: The case of the Shewhart X Chart. *Journal of Quality Technology*, 52(2), 198-217.

Jones-Farmer, L. A., Woodall, W. H., Steiner, S. H., & Champ, C. W. (2014). An overview of phase I analysis for process improvement and monitoring. *Journal of Quality Technology*, 46(3), 265-280.

Koutras, M. V., Triantafyllou, & S., I. (2020). *Distribution-Free Methods for Statistical Process Monitoring and Control.* Gewerbestrasse: Springer.

Krishnamoorthy, K., & Mathew, T. (2009). *Statistical tolerance regions: theory, applications, and computation*. John Wiley & Sons.

Mason, R. L., Tracy, N. D., & Young, J. C. (1995). Decomposition of T^2 for multivariate control chart interpretation. *Journal of quality technology*, 27(2), 99-108.

Montgomery, D. C. (2020). *Introduction to statistical quality control*. John Wiley & Sons.

Qin, S. J. (2012). Survey on data-driven industrial process monitoring and diagnosis. *Annual Reviews in Control, 36*(2), 220-234.

Qiu, P. (2014). *Introduction to statistical process control.* Boca Raton: CRC Press.

Qiu, P. (2018). Some perspectives on nonparametric statistical process control. *Journal of Quality Technology, 50*(1), 49-65.

Saleh, N. A., Mahmoud, M. A., Keefe, M. J., & Woodall, W. H. (2015). The difficulty in designing Shewhart X and X control charts with estimated parameters. *Journal of Quality Technology*, 47(2), 127-138.

Sultan, T. I. (1986). An acceptance chart for raw materials of two correlated properties. *Quality Assurance*, *12*(3), 70-72.

Wald, A. (1943). An Extension of Wilks' Method for Setting Tolerance Limits. *The Annals of Mathematical Statistics, 14*(1), 45-55.

Willemain, T. R., & Runger, G. C. (1996). Designing Control Charts Using an Empirical Reference Distribution. *Journal of Quality Technology, 28*(1), 31-38.

Wu, Z., Li, Y., Tsung, F., & Pan, E. (2023). Real-time monitoring and diagnosis scheme for IoT-enabled devices using multivariate SPC techniques. *IISE Transactions*, 55(4), 348-362.

Zhang, M., Megahed, F. M., & Woodall, W. H. (2014). Exponential CUSUM charts with estimated control limits. *Quality and Reliability Engineering International*, 30(2), 275-286.

Zhou, M., Zi, X., Geng, W., & Li, Z. (2015). A distribution-free multivariate change-point model for statistical process control. *Communications in Statistics-Simulation and Computation*, *44*(8), 1975-1987.

Author Biographies

Chase Holcombe is a PhD candidate in Applied Statistics at the University of Alabama. He holds an MS degree in Applied Statistics from the University of Alabama as well as a BS degree in mathematics and a BBA degree in economics from the University of North Alabama. His primary research interests are statistical process control, nonparametric statistical inference, and robust parametric methods to model and monitor integer-valued "count" processes. He is a member of the American Statistical Association.

Mosab Alqurashi is currently an Assistant Professor at the King Saud University (KSU, Saudi Arabia). He received his PhD degree in Applied Statistics from the University of Alabama. He also holds an MSc degree in Applied Statistics with specialization in business analytics from Bowling Green State University (BGSU, USA). His research interests are in statistical process control, nonparametric statistical inference, and operations research.

Subhabrata Chakraborti is Professor of Statistics and Robert C. and Rosa P. Morrow Faculty Excellence Fellow at the University of Alabama. He is a Fellow of the American Statistical Association and an Elected member of the International Statistical Institute. His current research interests are Nonparametric and Robust Statistical Inference methods with applications in areas such as Statistical Process Control, Survival/Reliability Analysis and Statistical Computing. He has extensive publications in peer-review journals and is a co-author of two books: *Nonparametric Statistical Inference* (2021), sixth edition, by CRC Press and *Nonparametric Statistical Process Control* (2019), by John Wiley and Sons. Professor Chakraborti serves as an Associate Editor of Communications in Statistics and Quality Engineering. He is a member of the American Statistical Association.

Appendix A

Let RL_0 and P denote the IC run length and probability of a false alarm respectively. We first derive the marginal probability mass function for RL_0. Note that as explained in the text, $RL_0|P \sim Geometric\ (P)$ and $P \sim Beta(k+1, m-k)$. Thus

$$\begin{aligned}
P(RL_0 = r) &= \int_0^1 f_{RL_0,P}(r,p)dp \\
&= \int_0^1 f_P(p) * f_{RL_0|P}(r|p)dp \\
&= \int_0^1 \frac{\Gamma(m+1)}{\Gamma(k+1)\Gamma(m-k)} p^{k+1-1}(1-p)^{m-k-1} * (1-p)^{r-1}p\ dp \\
&= \frac{\Gamma(m+1)}{\Gamma(k+1)\Gamma(m-k)} * \frac{\Gamma(k+2)\Gamma(m-k+r-1)}{\Gamma(m+r+1)} \\
&= \frac{m!\,(k+1)(m-k+r-2)!}{(m-k-1)!\,(m+r)!}, r = \{1,2,\dots\}
\end{aligned}$$

Next, we derive the CDF of RL_0.

$$\begin{aligned}
F_{RL_0}(r) &= \int_0^1 f_P(p) * F_{RL_0|P}(r|p)dp \\
&= \int_0^1 \frac{\Gamma(m+1)}{\Gamma(k+1)\Gamma(m-k)} p^{k+1-1}(1-p)^{m-k-1} * [1-(1-p)^{\lfloor r \rfloor}]dp \\
&= \int_0^1 f_P(p)dp - \int_0^1 \frac{\Gamma(m+1)}{\Gamma(k+1)\Gamma(m-k)} p^{k+1-1}(1-p)^{m-k-1} * (1-p)^{\lfloor r \rfloor}dp \\
&= 1 - \int_0^1 \frac{\Gamma(m+1)}{\Gamma(k+1)\Gamma(m-k)} p^{k+1-1}(1-p)^{m-k+\lfloor r \rfloor-1}dp \\
&= 1 - \frac{\Gamma(m+1)}{\Gamma(k+1)\Gamma(m-k)} * \frac{\Gamma(m-k+\lfloor r \rfloor)\Gamma(k+1)}{\Gamma(m+\lfloor r \rfloor+1)} \\
&= 1 - \frac{m!\,(m-k+\lfloor r \rfloor-1)!}{(m-k-1)!\,(m+\lfloor r \rfloor)!}, r \geq 1, 0\ otherwise
\end{aligned}$$

Next, we derive the expected value $E[RL_0]$ and the variance $Var[RL_0]$ of the IC run length distribution, using the expressions for the mean and the variance of the $RL_0|P$ distribution, which is geometric with parameter P

$$
\begin{aligned}
E[RL_0] &= EE[RL_0|P] \\
&= E\left[\frac{1}{P}\right] \\
&= \int_0^1 \frac{1}{p} * \frac{\Gamma(m+1)}{\Gamma(k+1)\Gamma(m-k)} p^{k+1-1}(1-p)^{m-k-1} dp \\
&= \int_0^1 \frac{\Gamma(m+1)}{\Gamma(k+1)\Gamma(m-k)} p^{k-1}(1-p)^{m-k-1} dp \\
&= \frac{\Gamma(m+1)}{\Gamma(k+1)} * \frac{\Gamma(k)}{\Gamma(m)} \\
&= \frac{m}{k} = ARL_0
\end{aligned}
$$

Finally, we derive the variance $Var[RL_0]$ using the result for $E[RL_0]$ and expressions for the mean and the variance of the $RL_0|P$ distribution, which is geometric, with parameter P.

$$
\begin{aligned}
Var[RL_0] &= E(Var[RL_0|P]) + Var(E[RL_0|P]) \\
&= E(Var[RL_0|P]) + E(E[RL_0|P])^2 - (EE[RL_0|P])^2 \\
&= \int_0^1 \left(\frac{1-p}{p^2}\right) * f_P(p) dp + \int_0^1 \frac{1}{p^2} * f_P(p) dp - \left(\frac{m}{k}\right)^2 \\
&= \int_0^1 \frac{2-p}{p^2} * f_P(p) dp - \left(\frac{m}{k}\right)^2 \\
&= 2\int_0^1 \frac{1}{p^2} * f_P(p) dp - \int_0^1 \frac{1}{p} * f_{P_0}(p) dp - \left(\frac{m}{k}\right)^2 \\
&= 2\int_0^1 \frac{1}{p^2} * \frac{\Gamma(m+1)}{\Gamma(k+1)\Gamma(m-k)} p^{k+1-1}(1-p)^{m-k-1} - \frac{m}{k} - \left(\frac{m}{k}\right)^2 \\
&= 2 * \frac{(k-2)!\, m!}{k!\,(m-2)!} - \frac{m}{k} - \left(\frac{m}{k}\right)^2 \\
&= \frac{m(k+1)(m-k)}{k^2(k-1)}
\end{aligned}
$$

Appendix B

The distribution of the IC conditional average run length ($CARL_0$)

Since the IC conditional distribution $RL_0|P$ is $Geometric\ (P)$, the mean of the IC conditional distribution, $CARL_0 = Y = \frac{1}{P}$ where $P \sim Beta(k+1, m-k)$.

Now $F_Y(y) = P(Y \leq y) = P\left(\frac{1}{P} \leq y\right) = P\left(P > \frac{1}{y}\right) = 1 - P\left(P \leq \frac{1}{y}\right) = 1 - F_P(\frac{1}{y})$

Thus,

$$
\begin{aligned}
f_{CARL_0}(r) &= \frac{\partial}{\partial y} F_P\left(\frac{1}{y}\right) \\
&= \frac{\Gamma(m+1)}{\Gamma(k+1)\Gamma(m-k)} \left(\frac{1}{r}\right)^{k+1+2-1} \left(1-\frac{1}{r}\right)^{m-k-1} \\
&= \frac{\Gamma(m+1)}{\Gamma(k+1)\Gamma(m-k)}\ r^{-(m+1)}(r-1)^{m-k-1}, r \geq 1, k < m
\end{aligned}
$$

Now, we turn our attention to deriving $E[CARL_0]$ and $Var[CARL_0]$. The derivation for $E[CARL_0]$ is very straightforward since it is equal to $E[RL_0]$, both of which are equal to ARL_0 .

$$
\begin{aligned}
E[CARL_0] &= E[RL_0] \\
&= \mathrm{E}\left[\frac{1}{P}\right] \\
&= \frac{m}{k} = ARL_0
\end{aligned}
$$

Similarly, $Var[CARL_0]$ may be derived using the distribution of P.

$$
\begin{aligned}
Var[CARL_0] &= Var\left[\frac{1}{P}\right] \\
&= E\left[\frac{1}{P^2}\right] - \left(E\left[\frac{1}{P}\right]\right)^2 \\
&= \int_0^1 \frac{1}{p^2} * \frac{\Gamma(m+1)}{\Gamma(k+1)\Gamma(m-k)} p^{k+1-1}(1-p)^{m-k-1} dp - \left(\frac{m}{k}\right)^2
\end{aligned}
$$

$$= \frac{m(m-1)}{k(k-1)} - \left(\frac{m}{k}\right)^2$$

$$= \frac{m(m-1)k - m^2(k-1)}{k^2(k-1)}$$

$$= \frac{m(m-k)}{k^2(k-1)}$$

Appendix C

Table 9: Simulated Data Points

Sample Number	X_1	X_2	X_3	Sample Number	X_1	X_2	X_3
1	-0.6633	1.3460	3.4886	**41**	3.0253	0.5503	2.0825
2	-1.0960	0.6749	1.9976	**42**	2.9422	0.9019	1.9661
3	0.8147	1.4505	3.9202	**43**	4.2436	1.7602	1.1141
4	0.0664	1.6018	3.0368	**44**	4.9242	0.3377	0.8470
5	-0.4655	0.3760	3.4180	**45**	3.3881	1.0949	2.1401
6	-2.0024	1.2515	2.0300	**46**	3.4019	-0.1307	1.1069
7	1.2871	2.1819	4.2206	**47**	5.1731	1.3487	1.6118
8	-0.5675	2.6756	4.1644	**48**	2.8794	0.1558	0.2522
9	-0.5632	-1.1718	1.8459	**49**	3.4605	0.4764	2.8851
10	-0.3480	1.6639	2.4195	**50**	4.8463	0.9013	0.9853
11	0.8963	1.7531	3.1883	**51**	5.1516	2.2045	3.0019
12	-0.5262	0.0533	1.2040	**52**	4.6897	1.0320	2.6629
13	-1.9430	-0.4166	1.0676	**53**	5.1669	1.1162	1.1927
14	-0.5240	0.0887	-0.0071	**54**	4.9315	1.8566	1.9752
15	-0.2733	2.7251	2.9947	**55**	5.4711	0.7699	2.3016
16	1.8323	1.1904	2.0294	**56**	1.8872	0.5640	2.8285
17	-0.5592	-0.3772	0.8743	**57**	3.4066	0.2272	2.4305
18	1.9734	1.3116	3.2887	**58**	3.1184	0.6116	0.3149
19	-1.5330	-1.1817	1.0945	**59**	2.4262	-0.0372	0.7518
20	1.3493	2.7186	3.9865	**60**	5.4656	2.0025	1.6060
21	-1.2818	2.2752	1.6579	**61**	4.8074	2.0665	2.5327
22	0.1995	1.3076	1.3524	**62**	4.5865	2.0658	1.8653
23	-2.0372	0.0721	1.7667	**63**	3.7106	1.4652	0.9570
24	-1.0613	-0.0031	2.0004	**64**	4.2169	1.1344	2.4602
25	-0.0327	1.3577	2.0434	**65**	5.0760	1.5647	2.3898
26	-0.4721	2.1850	2.9819	**66**	5.0623	2.4215	2.7469
27	0.7573	0.1947	2.7083	**67**	3.1777	1.0406	3.5364
28	-1.9004	-0.2675	0.3798	**68**	3.9522	1.8625	3.3177
29	-1.7336	1.9870	1.6126	**69**	4.7848	1.2479	2.2867
30	-0.3336	0.6637	2.2478	**70**	3.1702	0.9670	1.1703
31	1.8477	2.6765	1.4367	**71**	2.8663	-0.3028	1.0420
32	-1.8093	-1.0689	0.2820	**72**	4.9104	0.8809	1.9365
33	1.8073	1.2870	1.3807	**73**	3.7810	1.6235	2.9880
34	-0.2845	1.9194	2.4618	**74**	3.9137	1.4234	1.7442
35	-0.5743	0.0042	0.9512	**75**	5.2642	2.0820	3.2333
36	2.4034	2.8954	4.3693	**76**	4.4532	0.8702	0.2830
37	-0.5936	0.3089	0.8816	**77**	3.4181	1.1631	1.6083
38	0.0090	1.7190	3.4028	**78**	3.7842	0.9487	3.4284
39	0.7773	1.8762	3.3547	**79**	3.1933	0.3992	1.8301
40	1.0555	1.1908	1.3837	**80**	4.2503	1.2181	2.0200